

Strong Photoluminescence Enhancement from Colloidal Quantum Dot Near Silver Nano-Island Films

Hagen Langhuth · Simon Frédérick ·
Michael Kaniber · Jonathan J. Finley ·
Ulrich Rührmair

Received: 15 August 2010 / Accepted: 28 September 2010 / Published online: 9 October 2010
© Springer Science+Business Media, LLC 2010

Abstract We present the fabrication and optical investigation of highly random self-assembled, nano-scale films, probing their influence on the luminescence properties of near surface CdSe/ZnS colloidal quantum dots. When compared to quantum dots distributed on unstructured quartz substrates, the average luminescence intensity is found to be enhanced by a factor of $160\times$. The silver nanoparticles are prepared using slow thermal evaporation on quartz substrates and post-deposition annealing to produce a randomly-arranged layer of smooth nano-islands. Clear polarization dependent hot spots are observed. Such hot spots deliver a maximal enhancement of the emission intensity of $240\times$ and have a spatial density of $(0.050\pm 0.002)\ \mu\text{m}^{-2}$. The results show that silver nano-island films strongly enhance the optical efficiency of near quantum dots emitters.

Keywords Quantum dots · Silver nano-islands · Self-assembled films · Plasmonic hot spots · Surface sensing

Recent advances in plasmonics have renewed interest in the study of the optical properties of thin metallic

films. A non-uniform metallic film, patterned on the nano-scale either by advanced electron-beam lithography techniques [1–4] or formed via self-assembly [5–10], can dramatically modify the optical properties of a material in its vicinity. For example, such metallic nanostructures can enhance the absorption strength of proximal or embedded optical materials to realize high efficiency solar cells [1, 2, 6, 9]. The concentrated electric field produced by hot spots in such nanoscale metallic structures can also lead to large modifications of the spontaneous emission properties [4–6, 11] and, even, suppress fluorescence intermittency [12, 13] and reduce device fatigue [11, 13].

In this letter, we use a simple technique to produce silver nano-island films by combining slow evaporation and rapid thermal annealing. Our approach produces smooth half-spheroid silver nano-islands, in strong contrast with chemistry-based techniques that typically produce arrays of spheres [7, 8, 14]. It has recently been shown that half-spheroid metallic nanoparticles scatter the incident light more efficiently into surface plasmon polariton modes, thus coupling more efficiently to the adjacent material; colloidal CdSe/ZnS quantum dots (QDs) in our case [15]. At a controlled separation of 10 nm between the QD layer and the silver film, very large enhancements of the luminescence intensities are observed; an average enhancement factor (η) of $160\times$ being observed with specific hot spots yielding $\eta \geq 240\times$.

The silver nano-island films used in this work were prepared by slow thermal evaporation of a nominally 10 nm-thick silver layer onto a quartz substrate at 10^{-6} mbar. After deposition, the samples were rapid-thermal-annealed at $250\ ^\circ\text{C}$ in a forming gas atmosphere for 10 min. Figure 1a shows a typical atomic

H. Langhuth · S. Frédérick (✉) · M. Kaniber · J. J. Finley
Walter Schottky Institut, Technische Universität München,
Am Coulombwall 3, 85748 Garching bei München, Germany
e-mail: sim.frederick@gmail.com

U. Rührmair
Institut für Informatik, Technische Universität München,
Boltzmannstr. 3, 85748 Garching bei München, Germany

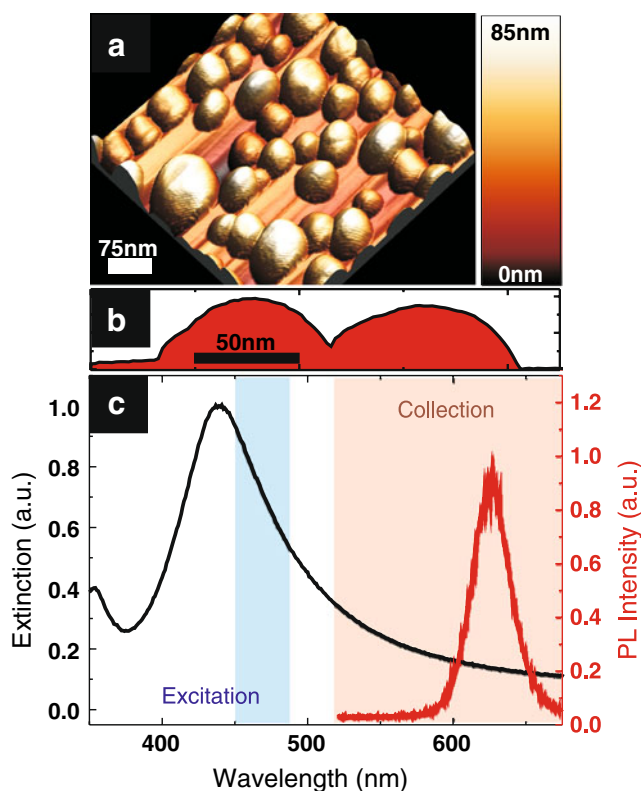


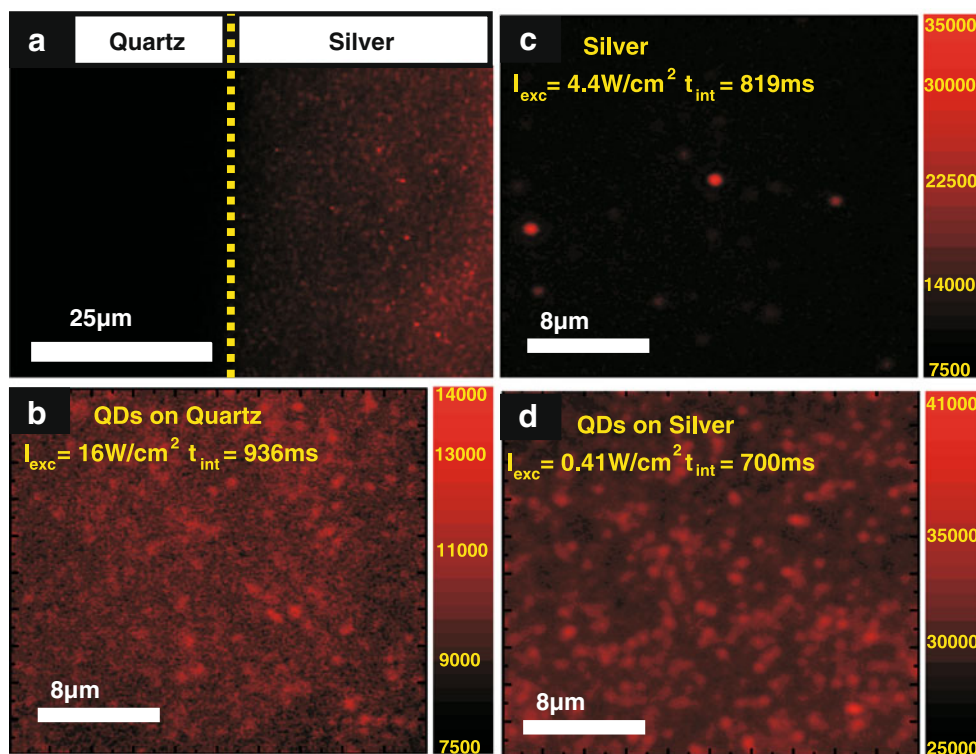
Fig. 1 **a** Atomic force microscopy image of typical silver nano-island film used in this work. **b** Surface profile of two adjacent islands. **c** Typical silver nano-island film extinction spectra (black line) and CdSe/ZnS typical photoluminescence spectra (red line). The shaded blue and red areas highlight the spectral dependence of the excitation and collection filters respectively

force microscopy (AFM) image of the obtained surface. The nano-islands formed by this technique are smooth (surface roughness <0.5 nm) half-spheroids as shown in the surface profile in Fig. 1b. They have a broad Gaussian distribution of diameters and heights, with an average diameter of 50 nm. The full-width at half maximum (FWHM) of this distribution is 40 nm whereas the height is centered at 37 nm with a FWHM of 20 nm. The islands have an areal density of $230 \pm 10 \mu\text{m}^{-2}$. From these values we estimate an average inter-island distance of (16.0 ± 0.7) nm. However, the random assembly process produces a broad distribution in terms of inter-island separation ranging from adjacent islands to distances >100 nm. After nano-island growth a 10 nm-thick layer of SiO_2 is deposited by sputtering to serve as a spacer between the silver and the QDs. This allows the QDs to be brought into the near field of the electric field associated with plasmonic resonances whilst preventing luminescence quenching due to charge transfer between the QDs and the silver nanoparticle surface [4, 5]. The extinction spectra of the sample, measured

using a Xenon lamp in a Varian Cary 50 microscope system, is presented as the black curve in Fig. 1c. The broad peak spanning the region 400–500 nm with a peak wavelength at 440 nm is the ensemble-averaged plasmon resonance of the silver nanoparticles. This wavelength is fully consistent with expectations, given the ~ 50 nm lateral size of the islands [9, 13].

The colloidal QDs used in this study have CdSe core with a ZnS shell (CdSe/ZnS). They were dispersed on the silver nano-island film by dilution in Toluene to a concentration of 12 nM and spinning them at 4,000 rpm for 40 s. The red curve in Fig. 1c shows a typical QD ensemble photoluminescence spectra recorded by exciting with a 405 nm laser with a power density of 70 W/cm^2 . It shows a strong peak centered at 625 nm. We note that the plasmon resonance at 440 nm overlaps strongly with the absorption spectrum of the CdSe/ZnS QDs. We used an Axiovert 200M MAT fluorescence microscope from Zeiss with an ORCA ER Hamamatsu camera to image the resulting fluorescence from our sample. Filters inserted in the microscope select the excitation wavelength range from a mercury vapor lamp to be 450 to 490 nm as illustrated by the blue shaded area in Fig. 1c. Hence, the excitation light is absorbed not only by the quantum dots but also excites plasmons in the silver nano-island film. The red shaded area in Fig. 1c depicts schematically the wavelength range that is detected by the silicon CCD detector (>515 nm), as selected by a long-pass filter. Figure 2a shows a typical image of an area of the sample containing both QDs on bare quartz (left panel) and on the silver nano-island film (right panel). The QDs in the vicinity the silver nano-island film clearly emit more strongly than those on the bare quartz. This is due to the combined effects of the enhanced absorption by the silver nano-island film and an increased radiative decay rate due to coupling of the QDs to plasmonic radiative modes where the electric field is enhanced. The excitation power density (I_{exc}) is varied between 0.41 and 16 W/cm^2 whilst the integration time (t_{int}) is adjusted between 0.7 and 1.0 s to properly image the different samples. Figure 2b shows the normalized QD photoluminescence intensity on quartz and the silver film luminescence is displayed in Fig. 2c. We attribute this luminescence to photoactivated emission in nanoscale silver oxide [16]. Finally, Fig. 2d shows the luminescence of QDs on a silver nano-island film. In this case, most of the energy absorbed by the silver nano-islands will be extracted from the sample by photon emission via QDs. Those images were normalized by taking the number of counts for each pixel and dividing it by the excitation intensity and the integration time. The average

Fig. 2 **a** Photoluminescence of QDs lying on bare quartz (*left*) and a silver nano-islands film (*right*) area. Normalized photoluminescence of **b** QDs lying on bare quartz, **c** the silver nano-island film, and **d** QDs lying on silver nano-islands film



normalized pixel intensities are measured to be 650, 2,800, and 105,000 counts/(J/cm²) for the QDs on the quartz substrate, the silver nano-islands without QDs and the silver nano-islands and QDs, respectively. Subtracting of the average intensity of the silver luminescence from the QD-coated sample shows an average 160× enhancement of the QD luminescence intensity with respect to their luminescence on bare quartz. This value is the average enhancement, each pixel containing more than 100 QDs.

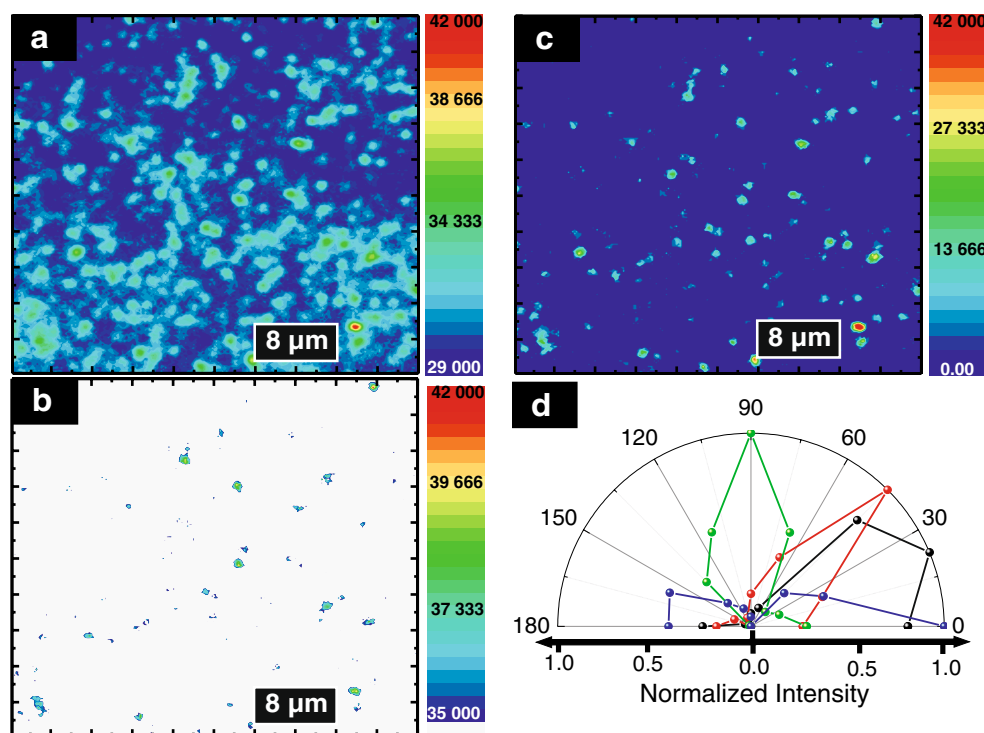
The granular nature of the QD luminescence on the quartz substrate is attributed to the formation of QD aggregates. Whilst aggregates also form when the QDs are spun onto a silver substrate, a study of their polarization dependence reveals the presence of hot spots with well defined polarization. Figure 3a shows a false color image of the QD photoluminescence on a silver nano-island film with unpolarized excitation. The insertion of a linear polarizer into the excitation beam path confirms that the higher intensity light-granules stem from plasmonic hot spots and are not simply QD aggregates. Most of the high intensity occurrences exhibit a clear linear polarization dependence. Figure 3b shows the photoluminescence of the same sample area whilst exciting with a linearly polarized light. Pixels with an intensity below 83% of the maximum pixel intensity were set to zero in order to highlight only the high intensity

events. We apply this same numerical *flooding* process¹ for a range of linear polarizations from 0 to 180° in steps of 22.5°. The multiplication of all these images yields a featureless image, confirming that each of the high intensity centers are linearly polarized. Figure 3c shows the sum of all the polarization dependent images divided by the number of images. This procedure allows us to clearly identify the position of the hot spots and evaluate their polarization dependence individually. The hot spot density is (0.050±0.002) μm⁻². Each hot spot reaches a maximum value at a unique polarization angle. The normalized hot spot intensity as a function of the polarization angle is presented in Fig. 3d for four different, but typical, hot spots.

The average of all of the polarization-dependent maximum pixel values is 130,000 counts/(J/cm²). On the other hand, the average hot spot normalized pixel intensity for the silver films without any QDs is 3,900 counts/(J/cm²). Thus, the average hot spot-induced QD photoluminescence enhancement is 190× the average value for QDs on bare quartz. The best pixel in the best hot spot yields a luminescence enhancement $\eta = 240\times$. These values are strikingly

¹This numerical procedure sets all pixels with an intensity inferior to the specified threshold to zero.

Fig. 3 False color plot of the colloidal quantum dot photoluminescence on a silver nano-island film: **a** Un-polarized, **b** linearly polarized, and **c** sum of all the linearly polarized luminescence images. **d** Normalized intensity of individual high-intensity photoluminescence hot spots as a function of the excitation linear polarization angle. The hot spot intensity has been normalized with respect to its maximum (I_{\max}) and minimum intensity (I_{\min})



higher than those reported for films defined using electron beam lithography [4].

We believe the linearly polarized hot spots originate from small gaps (few nanometers) between two or more adjacent silver nano-islands. An example of such a situation is shown on Fig. 1b. It has been shown that such plasmonic dimers can generate very strong local field enhancements where the emitter quantum efficiency is greatly increased due to the combination of the Purcell effect and an enhanced absorption cross-section [2, 17, 18]. Moreover, it was shown in Ref. [18] that arrays of metallic nano-particles can generate even higher spontaneous emission rate enhancements. Whilst the average distance between neighboring nano-islands is ≈ 16 nm, it is clear from the random film formation process that smaller distances occur in our experiment. This expectation is confirmed by the AFM measurement presented in Fig. 1a. Moreover, the highest local field enhancement is not produced for the smallest inter-island spacing, but for an optimal value that depends on the wavelength, and dielectric constants of the metal and surrounding material [2, 17]. The low density of hot spots (0.050 ± 0.002) μm^{-2} compared to the density of silver nano-islands (230 ± 10) μm^{-2} is in good agreement with the nano-island formation process and the resulting Gaussian distribution of the nano-island sizes and positions.

In conclusion, we produced high quality silver-based plasmonic films with smooth half-spheroidal nano-

islands. With a 10 nm-thick SiO_2 spacer, the photoluminescence of a layer of CdSe/ZnS colloidal QDs is enhanced on average by a factor of $\eta = 160$ compared to a nominally equal layer on bare quartz. We also observed the formation of polarization-dependent hot spots where the photoluminescence is on average enhanced by $\eta = 190$ and maximally $\eta = 240$. The hot spots are believed to occur in gaps between nano-islands where two or more islands are coupled to generate very large electric fields.

Acknowledgements This project was supported by the Deutsche Forschungs Gemeinschaft via the Nanosystems Initiative Munich. SF acknowledges support from the Alexander von Humboldt Foundation.

References

1. Ferry VE, Verschuuren MA, Li HBT, Schropp REI, Atwater HA, Polman A (2009) Improved red-response in thin film a-Si:H solar cells with soft-imprinted plasmonic back reflectors. *Appl Phys Lett* 95:183503
2. Shen H, Bienstman P, Maes B (2009) Plasmonic absorption enhancement in organic solar cells with thin active layers. *J Appl Phys* 106:073109
3. Hugall JT, Baumberg JJ, Mahajan S (2009) Surface-enhanced raman spectroscopy of CdSe quantum dots on nanostructured plasmonic surfaces. *Appl Phys Lett* 95:141111
4. Pompa PP, Martiradonna L, Della Sala A, Manina L, De Vittorio M, Calabi F, Cingolani R, Rinaldi R (2006)

- Metal-enhanced fluorescence of colloidal nanocrystals with nanoscale and control. *Nature Nanotechnology* 1:126
5. Ozel T, Soganci IM, Nizamoglu S, Huyal IO, Mutlugun E, Sapra S, Gaponik N, Eychmüller A, Demir HV (2008) Selective enhancement of surface-state emission and simultaneous quenching of interband transition in white-luminophor cds nanocrystals using localized plasmon coupling. *New J Phys* 10:083035
 6. Soganci IM, Nizamoglu S, Mutlugun E, Akin O, Demir HV (2007) Localized plasmon-engineered spontaneous emission of cdse/zns nanocrystals closely-packed in the proximity of ag nanoisland films for controlling emission linewidth, peak, and intensity. *Opt Express* 15:14289
 7. Banerjee R, Hazra S, Banerjee S, Sanyal MK (2009) Nanopattern formation in self-assembled monolayers of thiol-capped au nanocrystals. *Phys Rev E* 80:056204
 8. Aslan K, Malyn SN, Zhang Y, Geddes CD (2008) Conversion of just-continuous metallix films to large particulate substrates for metal-enhanced fluorescence. *J Appl Phys* 103:084307
 9. Beck FJ, Polman A, Catchpole KR (2009) Tunable light trapping for solar cells using localized surface plasmons. *J Appl Phys* 105:114310
 10. Komarala VK, Bradley AL, Rakovich YP, Byrne SJ, Gun'ko YK, Rogach AL (2008) Surface plasmon enhanced Förster resonance energy transfer between the cdte quantum dots. *Appl Phys Lett* 93:123102
 11. Borys NJ, Walter MJ, Lupton JM (2009) Intermittency in second-harmonic generation radiation from plasmonic hot spots on rough silver film. *Phys Rev B* 80:161407(R)
 12. Fu Y, Zhang J, Lakowicz JR (2007) Suppressed blinking in single quantum dots (QDs) immobilized near silver island films (SIFs). *Chem Phys Lett* 447:96
 13. Lakowicz JR, Ray K, Chowdhury M, Szymanski H, Fu Y, Zhang J, Nowaczyk K (2008) Plasmon-controlled fluorescence: a new paradigm in fluorescence spectroscopy. *Analyst* 133:1308
 14. Komarala VK, Rakovich YP, Bradley AL, Byrne SJ, Gun'ko YK (2006) Off-resonance surface plasmon enhanced spontaneous emission from CdTe quantum dots. *Appl Phys Lett* 89:253118
 15. Catchpole KR, Polman A (2008) Design principles for particle plasmon enhanced solar cells. *Appl Phys Lett* 93:191113
 16. Peyser LA, Vinson AE, Bartko AP, Dickson RM (2001) Photoactivated fluorescence from individual silvernanoclusters. *Science* 291:103
 17. Ringler M, Schwemer A, Wunderlich M, Nichtl A, Kürzinger K, Klar TA, Feldmann J (2008) Shaping emission spectra of fluorescent molecules with single plasmonic nanoresonators. *Phys Rev Lett* 100:203002
 18. Muskens OL, Giannini V, Sánchez-Gil JA, Gómez Rivas J (2007) Strong enhancement of the radiative decay rate of emitters by single plasmonic nanoantennas. *Nanoletters* 7:2871